Internal Compton effect in ^{113}In†

M. Jurčević, K. Ilakovac, and Z. Krečak
Institute Rudjer Bošković, Zagreb, Yugoslavia
(Received 20 November 1974)

Previous measurements of the $e\gamma$ double decay of ^{113}In at 35° have been extended to relative angles of emission of 15, 30, 45, 60, 90, 120, and 150°. The energy distributions of photons have been determined at each angle in the range from 30 to 210 keV and from 35 to 197 keV for $K\gamma$ and $(L+M+N)\gamma$ decays, respectively. The data are in agreement with the theory of the internal Compton effect of Spruch and Goertzel and the theory of radiation losses in internal conversion of Baumann and Robl. The maximum of the transition probability has been found at $(39.8\pm2.2)°$, while that predicted by the theories is at 34.6°. The calculations have also been performed using the theory of "nuclear" $e\gamma$ double decay of Grechukhin. It has been shown that the contributions of this mechanism to the observed results are negligible. The integral coefficients obtained are $B_{K\gamma} = (1.11\pm0.04)\times10^{-3}$ for photons in the energy range from 35 to 105 keV and $B_{(L+M+N)\gamma} = (1.01\pm0.08)\times10^{-3}$ for photons in the energy range from 42 to 105 keV.

RADIOACTIVITY ^{113}In^m; measured $e\gamma$ double decay at 15, 30, 35, 45, 60, 90, 120, and 150°; deduced photon energy distributions in the range 30 to 210 keV for $K\gamma$ decay and 35 to 197 keV for $(L+M+N)\gamma$ decay; deduced angular distribution for photons of an energy of 35 to 105 keV for $K\gamma$ decay and 42 to 105 keV for $(L+M+N)\gamma$ decay; deduced integral energy distribution and integral $e\gamma$–double-decay coefficients.

INTRODUCTION

The results of measurements of the electron-photon double decay ($e\gamma$ decay) of the 392-keV isomeric state in ^{113}In at a relative angle of emission of 35° were presented in a previous paper[1] (hereafter referred to as I). The continuous energy distributions of photons from $e\gamma$ decay were compared with the coefficients of the internal Compton effect (ICE) derived from the theory of Spruch and Goertzel.[2] The experimental results are in good absolute agreement with the theoretical predictions. In this paper we present the results of measurements performed with the aim of determining the angular and energy distributions in the $e\gamma$ decay of ^{113}In. We also performed a more detailed comparison of the experimental data with several theories of $e\gamma$ decay.

MEASUREMENTS

The apparatus and the method of measurement were described in detail in I. Here we present only the main features and modifications.

Photons and electrons from $e\gamma$ decay continuously share the available energy, i.e.,

$$E + E_e = W_0 - B_e , \quad (1)$$

where E and E_e are the energies of the emitted photon and electron, respectively, W_0 is the transition energy, and B_e is the binding energy of the electron. The recoil energy of the atom is neglected. The identification of $e\gamma$ events was based on the energy condition in Eq. (1) and on the condition of simultaneity. A three-dimensional 256-256-256-channel analyzer was used to record the amplitudes of pulses from the photon and electron detectors, and from a time-to-amplitude converter which measured the time difference.

New measurements were performed at seven nominal angles, $\Theta_0 = 15$, 30, 45, 60, 90, 120, and 150°. The arrangement used in the measurements was the same as that described in I. For comparison, we repeat the results of the previous measurement at a nominal angle of 35°. A silicon surface-barrier detector of a sensitive area of 12 mm in diameter was used in the measurements at 15, 30, and 35°, whereas a silicon surface-barrier detector of a sensitive area of 14 mm in diameter was employed in the measurements at 45, 60, 90, 120, and 150°. The energy resolution of these detectors was between 6 and 8 keV for K conversion electrons of 364 keV emitted in the decay of ^{113}In. A coaxial Ge(Li) detector of a sensitive volume of 25 cm^3 (detector A in I) was used to detect photons.

The time resolution of the system measured by coincident detection of K x rays and K conversion electrons emitted in the decay of ^{113}Sn was about 35 ns. The peak was asymmetrical, with a long "tail" caused by the delayed triggering of the photon discriminator. The time resolution of the fast

coincidence was set relatively large ($2\tau \approx 200$ ns) to avoid losses due to the tail and due to the shifts of the coincidence curve with energy.

The gain in the photon and electron branch was adjusted to have the same width per channel (1.5 keV/channel). The gain was rather stable over long periods of time (shifts were within ±0.25%).

The method of deriving the numbers of counts per channel in the photon branch from seven two-dimensional diagrams of sum energy versus photon energy, each corresponding to an interval of time difference of 32 ns, was described in I. From the counting rates we calculated the energy spectra of photons, which we attributed to $e\gamma$ double decay on the basis of arguments given in the following section.

EXTERNAL BREMSSTRAHLUNG

The external bremsstrahlung of conversion electrons in thin layers of materials, which were "viewed" by both the electron and photon detectors, satisfy the same energy and simultaneity conditions set in the measurements and analysis of $e\gamma$ decay. In order to estimate the contribution of the external bremsstrahlung in the source, it was decided to check whether the amount of $SnCl_2$ has an effect on the counting rates. A relative angle of emission of 60° was chosen, since it was estimated that at this angle the effect would be most readily observed. Therefore, in addition to the measurement with a source prepared by the standard procedure, a measurement with a "thick" source was made at a relative angle of emission of 60°. The preparation of the "thick" source was the same as that of the standard source, except that inactive $SnCl_2$ was added to a solution of radioactive $^{113}SnCl_2$ to increase its quantity by a factor of about 10. The activity (about 8 μCi), the thickness of the Zapon backing foil (about 100 $\mu g/cm^2$), and the size of the spot were almost the same.

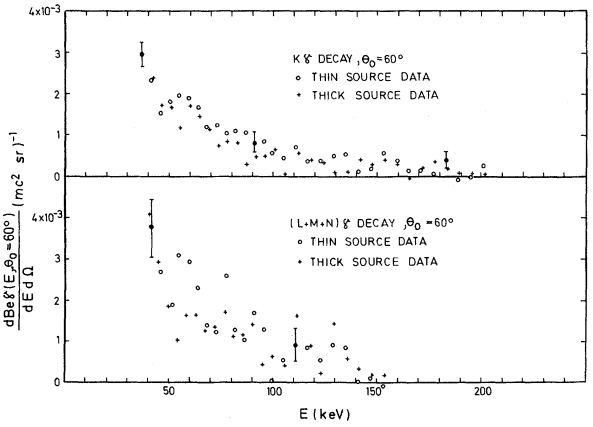

FIG. 1. Results of measurements of the $K\gamma$ and $(L+M+N)\gamma$ differential coefficients at $\Theta_0 = 60°$, with the "thick" and "thin" sources.

The results of measurements for $K\gamma$ and $(L+M+N)\gamma$ decays using the two sources are shown in Fig. 1. It can be seen that a tenfold increase of the $SnCl_2$ content in the source yielded no observable increase in the counting rates. After the integration over a photon-energy interval from 35 to 105 keV the following values for the $K\gamma$ differential coefficients were obtained: the "thick" source, $(1.70 \pm 0.16) \times 10^{-4}$ sr^{-1} and the standard source, $(1.98 \pm 0.14) \times 10^{-4}$ sr^{-1}. The difference amounts to $(-0.28 \pm 0.21) \times 10^{-4}$ sr^{-1}. These values indicate that the contribution of the external bremsstrahlung in $SnCl_2$ in the source is negligible (less than 1%).

This result is in agreement with the results obtained by Seykora,[3] who measured the external bremsstrahlung of 624-keV electrons in aluminum foils up to 200 mg/cm^2 thick.

The bremsstrahlung in the Zapon foils was estimated to be negligible because of its very small mass and because it is composed of light elements.

The bremsstrahlung of conversion electrons in the walls of the vacuum chamber (made of aluminum) also contributed to the counting rates in the region where $e\gamma$ events were expected. It was considerably reduced by lead shields placed around the photon detector. (The lead shields were used to prevent the Compton scattering of γ rays from the direct transition within the sensitive volume of the electron detector, with the detection of the secondary Compton photon in the photon detector.) The procedure of estimating upper limits of the counting rates for this process, on the basis of the counting rates at energies immediately below the sum energy of 364 keV, was explained in I.

TABLE I. Comparison of the calculated counting rates N_{brems} due to the external bremsstrahlung in the walls of the vacuum chamber with the observed counting rates N_{obs} for photons of energies between 50 and 150 keV. (The accuracy of the calculations of N_{brems} was estimated to be ±50%.)

Θ_0 (deg)	N_{brems}	N_{obs}	N_{brems}/N_{obs}
15	2.0 ± 1.0	156 ± 31	<3%
30	1.3 ± 0.65	942 ± 45	<0.2%
35	0.50 ± 0.25	913 ± 39	<0.1%
45	0.50 ± 0.25	654 ± 36	<0.15%
60	0.12 ± 0.06	863 ± 36	<0.03%
90	0.20 ± 0.10	385 ± 31	<0.1%
120	0.05 ± 0.03	122 ± 26	<0.05%
150	0.09 ± 0.05	73 ± 18	<0.20%

An upper limit of 3% was obtained at a relative angle of emission of 35°.

We also calculated the counting rates expected from the external bremsstrahlung in the parts of the vacuum chamber "viewed" by both detectors. From the stopping-power curve for electrons of 364 keV in aluminium we estimated that the effective thickness of the layer from which the contribution to the counting rates in the region of sum energy from 355 to 364 keV was possible, was about 20 μm. Taking into account the geometry of our experimental arrangement at each angle and the data of Aiginger[4] for the differential cross sections for the bremsstrahlung of electrons of 380 keV in aluminium, we estimated the counting rates in the region of photon energies from 50 to 150 keV. A comparison of the calculated counting rates with the observed ones is shown in Table I. The external bremsstrahlung in the walls of the vacuum chamber yields less than 0.3% to the counting rates observed at all angles except at 15°. In the measurement at a relative angle of emission of 15° the source had to be placed fairly far away from the detectors, and was only about 1 cm from the wall of the vacuum chamber. Owing to the proximity of the wall, the contribution of the external bremsstrahlung at this angle may be up to 3%.

Taking into account the above results and the accuracy of the measurements, we did not make corrections to the counting rates for external bremsstrahlung.

ANALYSIS OF MEASUREMENTS AND RESULTS

$K\gamma$ decay

The differential coefficients $dB_{e\gamma}(E,\Theta_0)/dE\,d\Omega$ for $e\gamma$ decay, defined as the ratios of the differential transition probabilities $dT_{e\gamma}(E,\Theta_0)/dE\,d\Omega$ for $e\gamma$ decay to the electron conversion transition probability T_e for the same shell, were calculated from the experimental spectra using Eq. (2) in I. The finite-geometry correction factor $C(E,\Theta_0)$ was calculated assuming the theoretical angular distribution of Spruch and Goertzel. Its value was close to 1 at all angles.

The efficiency of the Ge(Li) detector was checked several times in the course of measurements using a set of calibrated sources of ^{113}Sn, ^{57}Co, ^{241}Am, ^{22}Na, ^{137}Cs (supplied by the International Atomic Energy Agency, Vienna), and sources of ^{75}Se and ^{169}Yb.

The results for $K\gamma$ differential coefficients are given in Table II and in Figs. 2(a)–2(h). Table II gives averages taken over 12 channels ($\Delta E = 18$ keV), while Figs. 2(a)–2(h) show averages over different intervals of photon energy. The errors are the standard statistical errors. The full lines represent the theoretical values calculated from the theory of Spruch and Goertzel.[2] The values calculated from the theory of Baumann and Robl[5] are approximately equal to the values obtained from the former theory, and are not shown in these diagrams. In each figure averages were taken over the same photon energy intervals ΔE as the experimental data. The results of measurements obtained in the range of energy which was investigated are in good agreement with the theoretical values.

The angular distribution for $K\gamma$ decay obtained by integrating the experimental values of $K\gamma$ differential coefficients in the range of photon energy from 35 to 105 keV is given in Table IV (left column). These results are shown in Fig. 4(a). The full curves show the theoretical angular distribution derived from the theory of Spruch and Goertzel by integrating the differential internal Compton coefficients in the same range of photon energy.

TABLE II. $K\gamma$ differential coefficients $dB_{K\gamma}/dE\,d\Omega$ [in units of 10^{-3} $(mc^2\,sr)^{-1}$] in the $e\gamma$ decay of the 392-keV state in ^{113}In.

Photon energy interval (keV)	Relative angle of emission (Θ_0) 15°	30°	35°	45°	60°	90°	120°	150°
30–48	1.23± 0.29	2.60± 0.15	2.65± 0.15	3.19± 0.22	2.74± 0.17	0.63± 0.07	0.85± 0.15	0.08± 0.07
48–66	0.60± 0.19	1.71± 0.10	1.68± 0.12	1.91± 0.15	1.67± 0.10	0.40± 0.05	0.34± 0.05	0.09± 0.04
66–84	0.37± 0.18	1.12± 0.09	1.23± 0.11	1.35± 0.12	1.05± 0.09	0.28± 0.04	0.19± 0.07	0.07± 0.03
84–102	0.37± 0.16	0.60± 0.07	1.13± 0.10	0.81± 0.10	0.65± 0.07	0.21± 0.04	0.16± 0.06	0.07± 0.03
102–120	0.45± 0.19	0.48± 0.08	0.51± 0.07	0.59± 0.12	0.43± 0.06	0.18± 0.04	−0.03± 0.06	0.04± 0.04
120–138	0.13± 0.20	0.36± 0.07	0.31± 0.06	0.57± 0.11	0.34± 0.06	0.14± 0.04	0.20± 0.08	0.12± 0.05
138–156	0.33± 0.22	0.24± 0.08	0.43± 0.06	0.09± 0.11	0.34± 0.07	0.10± 0.04	−0.02± 0.09	−0.01± 0.01
156–174	0.75± 0.29	0.09± 0.09	0.31± 0.07	0.34± 0.12	0.18± 0.07	−0.02± 0.04	−0.05± 0.09	0.03± 0.05
174–192	0.42± 0.35	−0.02± 0.10	0.17± 0.07	0.54± 0.23	0.16± 0.08	0.04± 0.05	−0.11± 0.11	0.09± 0.06
192–210	−0.85± 0.45	0.00± 0.13	0.19± 0.08	0.00± 0.22	0.09± 0.11	−0.05± 0.09	−0.06± 0.13	0.03± 0.05

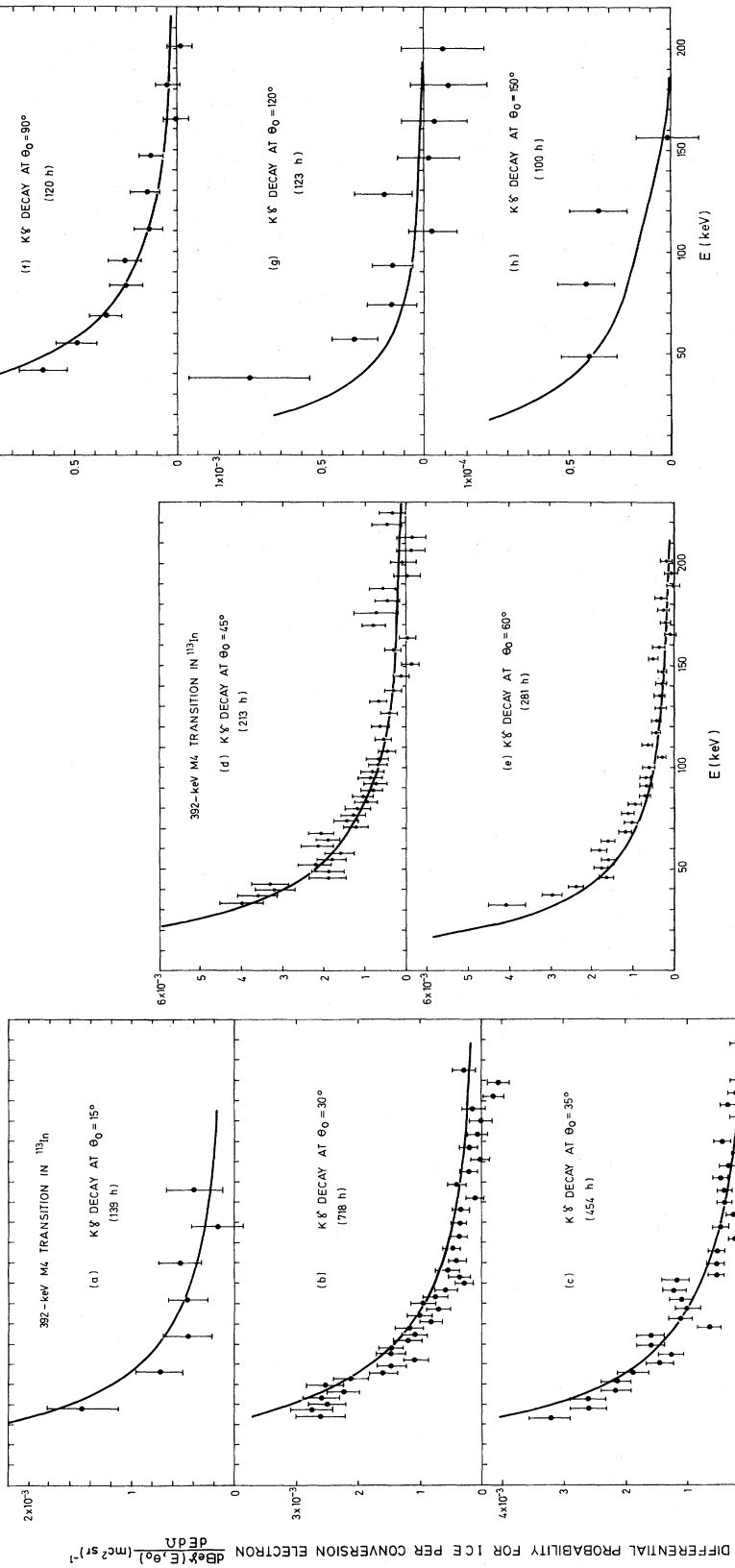

FIG. 2. Differential coefficients of $K\gamma$ decay in ^{113}In as a function of the photon energy E obtained in the measurements at several values of angle Θ_0. The solid lines were calculated from the theory of Spruch and Goertzel, which was modified by taking averages over energy intervals of the same width as the presented experimental data. (a) $\Theta_0=15°$, (b) $\Theta_0=30°$, (c) $\Theta_0=35°$, (d) $\Theta_0=45°$, (e) $\Theta_0=60°$, (f) $\Theta_0=90°$, (g) $\Theta_0=120°$, (h) $\Theta_0=150°$.

At relative angles smaller than 45° the theoretical values are (by small amounts) systematically larger than the experimental ones, but above 45° the deviation is in the opposite direction. A simple fitting procedure yielded the position of the maximum of the experimental angular distribution at $(39.8 \pm 2.2)°$, while the maximum of the theoretical curve is at 34.6°.

The integral $K\gamma$ coefficient, i.e. the ratio of the total $K\gamma$ transition probability for photon energies between 35 and 105 keV to the K conversion transition probability, was obtained by integrating the experimental angular distribution over the whole solid angle

$$B_{K\gamma}(E = 35 \text{ to } 105 \text{ keV}) = (1.11 \pm 0.04) \times 10^{-3}.$$

This value is in reasonable agreement with the values 1.09×10^{-3} and 0.91×10^{-3} calculated for the same photon energy interval from the theory of Spruch and Goertzel[2] and from the theory of Baumann and Robl,[5] respectively.

$(L+M+N)\gamma$ decay

The system (mainly the electron detector) did not allow the resolution of the sum-energy lines due to $L\gamma$, $M\gamma$, and $N\gamma$ double decays. From the experimental data (which were obtained along with the $K\gamma$ data) we calculated the differential coefficients for $(L+M+N)\gamma$ decay, i.e., the ratios of the differential transition probabilities for $L\gamma + M\gamma + N\gamma$ decay to the transition probability for $L+M+N$ electron conversion. The largest contribution to the process was estimated to be due to $L\gamma$ decay.

The results are given in Table III. These values were obtained by Eq. (2) in I. The intervals of photon energy of 18 keV were obtained by taking groups of 12 channels. The same data are shown in Figs. 3(a)–3(h); the averages of the data, however, were taken over different energy intervals.

To the knowledge of the authors, a calculation of the ICE involving $L, M, \ldots$-shell electrons has not been made as yet. Spruch and Geortzel have estimated the magnetic differential coefficients of the ICE for L electrons to be approximately equal to the magnetic differential coefficients for $K\gamma$ electrons for the same transition, i.e.,

$$dB_{L\gamma}(E, \Theta)/dE\, d\Omega \approx dB_{K\gamma}(E, \Theta)/dE\, d\Omega . \qquad (2)$$

Assuming this relation to be valid also for $M\gamma$ and $N\gamma$ decays, the differential coefficients for $(L+M+N)\gamma$ decay would be approximately equal to the differential coefficients for $K\gamma$ decay. The full lines in Figs. 3(a)–3(h) show the results calculated from the theory of Spruch and Geortzel for $K\gamma$ decay. The averages of these values were taken over the same intervals of photon energy as the experimental data.

The angular distribution of $(L+M+N)\gamma$ decay was calculated by integrating the experimental differential coefficients in an energy interval from 42 to 105 keV. The results are given in Table IV (right column) and shown in Fig. 4(b). The full line represents the differential coefficients of Spruch and Goertzel for the ICE integrated over the same range of photon energy. The agreement is not so good as for $K\gamma$ decay. The maximum of the angular distribution also appears at an angle that is somewhat larger than that given by the theory.

The integral coefficient for $(L+M+N)\gamma$ decay for an interval of photon energy from 42 to 105 keV,

$$B_{(L+M+N)\gamma}(E = 42 \text{ to } 105 \text{ keV}) = (1.01 \pm 0.08) \times 10^{-3},$$

was obtained by integrating the experimental angular distribution over the whole solid angle.

TABLE III. $(L+M+N)\gamma$ differential coefficients $dB_{(L+M+N)\gamma}/dE\, d\Omega$ [in units of 10^{-3} $(\text{mc}^2\,\text{sr})^{-1}$] in the $e\gamma$ decay of the 392-keV state in ^{113}In.

Photon energy interval (keV)	Relative angle of emission (Θ_0) 15°	30°	35°	45°	60°	90°	120°	150°
35–53	2.05 ± 0.78	4.01 ± 0.49	3.00 ± 0.37	4.19 ± 0.60	2.86 ± 0.31	0.76 ± 0.25	1.68 ± 0.35	0.09 ± 0.04
53–71	1.50 ± 0.63	2.18 ± 0.33	2.13 ± 0.26	1.84 ± 0.37	1.80 ± 0.21	0.54 ± 0.13	0.29 ± 0.23	0.05 ± 0.03
71–89	0.83 ± 0.63	0.70 ± 0.24	1.34 ± 0.22	1.60 ± 0.32	1.18 ± 0.19	0.31 ± 0.11	−0.10 ± 0.23	0.03 ± 0.03
89–107	0.06 ± 0.54	0.80 ± 0.22	1.02 ± 0.20	0.38 ± 0.23	0.82 ± 0.16	0.43 ± 0.14	0.35 ± 0.25	0.06 ± 0.03
107–125	0.04 ± 0.68	0.51 ± 0.24	0.29 ± 0.11	0.49 ± 0.23	0.86 ± 0.17	0.22 ± 0.13	0.36 ± 0.22	0.07 ± 0.03
125–143	0.32 ± 0.78	0.25 ± 0.24	0.59 ± 0.33	0.44 ± 0.24	0.67 ± 0.17	0.15 ± 0.13	0.71 ± 0.27	0.05 ± 0.04
143–161	0.98 ± 0.98	0.65 ± 0.28	0.20 ± 0.17	0.10 ± 0.34	0.37 ± 0.19	0.35 ± 0.15	−0.04 ± 0.34	0.08 ± 0.04
161–179	−0.75 ± 1.20	−0.17 ± 0.47	0.29 ± 0.19	0.30 ± 0.37	0.92 ± 0.23	−0.30 ± 0.19	0.46 ± 0.39	0.18 ± 0.06
179–197	−1.41 ± 1.39	−0.22 ± 0.47	0.54 ± 0.21	−0.92 ± 0.50	0.26 ± 0.41	0.07 ± 0.20	0.07 ± 0.41	0.06 ± 0.06

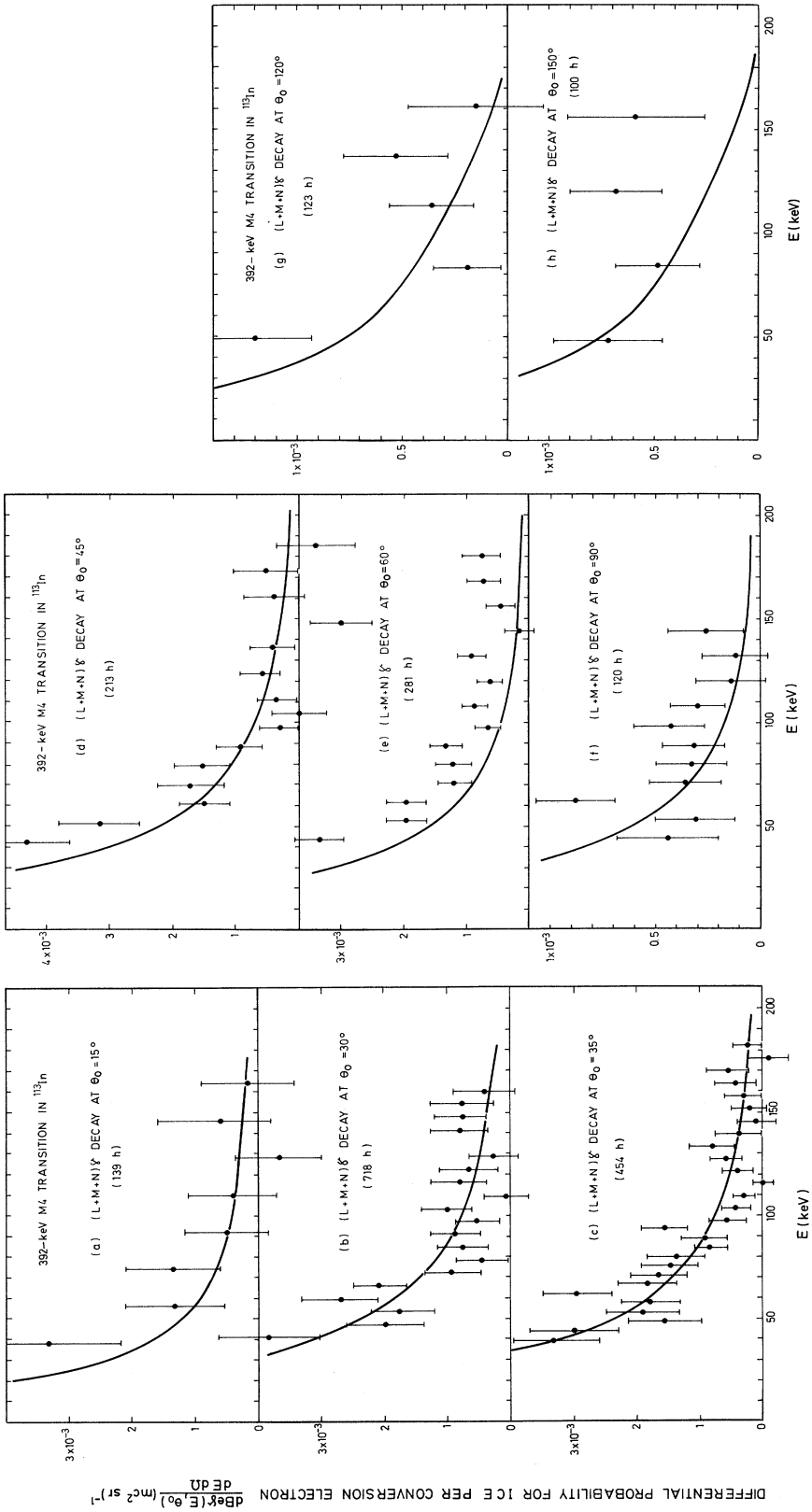

FIG. 3. Differential coefficients of $(L+M+N)\gamma$ decay in ^{113}In as a function of the photon energy E obtained in the measurements at several values of angle Θ_0. The solid lines were calculated from the theory of Spruch and Goertzel using formula (2) which was modified by taking averages over energy intervals of the same width as the presented experimental data. (a) $\Theta_0=15°$, (b) $\Theta_0=30°$, (c) $\Theta_0=35°$, (d) $\Theta_0=45°$, (e) $\Theta_0=60°$, (f) $\Theta_0=90°$, (g) $\Theta_0=120°$, (h) $\Theta_0=150°$.

DISCUSSION

$e\gamma$ decay is a type of higher-order electromagnetic transition. This process in lowest order can proceed via electronic or nuclear virtual intermediate states. The two mechanisms differ in that the real photon is emitted by the electron or by the nucleus, respectively.

Electronic intermediate states

Several authors[2,5,6-12] have calculated the rates and shapes of continuous spectra of electromagnetic radiation emitted by outgoing electrons in nuclear decay. Here we discuss only those papers the results of which we applied in the analysis of the data.

A simple, semiclassical theory of the internal bremsstrahlung in β decay was developed by Wang Chang and Falkoff.[6] They calculated the radiation of an electron created in the nucleus at some instant, with the assumption that the velocity of the electron is constant at all later times.

The radiation of conversion electrons has been studied by several authors.[2,5,7-12] It is usually called the ICE.

Spruch and Goertzel calculated the magnetic ICE differential coefficients for K-shell electrons, i.e., the ratios of the transition probability per unit solid angle and unit energy interval for $K\gamma$ decay to the transition probability for K electron conversion, for magnetic multipole transitions. The initial state of the electron was described by a nonrelativistic wave function, and the intermediate and final states by plane waves. The results of a similar approximation for the transition probability of K electron conversion were applied. In both calculations a point nucleus was assumed, so the nuclear matrix elements cancelled. In taking the ratio the errors seem to have cancelled to a high degree because of the application of similar approximations. This may be inferred from the agreement of the theory with the energy and angular distributions in the $K\gamma$ decay of ^{137}Ba[13] and with the present measurements of ^{113}In. The value of the K conversion coefficient for the 392-keV $M4$ transition in ^{113}In calculated in the Born approximation (as used by Spruch and Goertzel) is 0.14. This is about one-third of the experimental

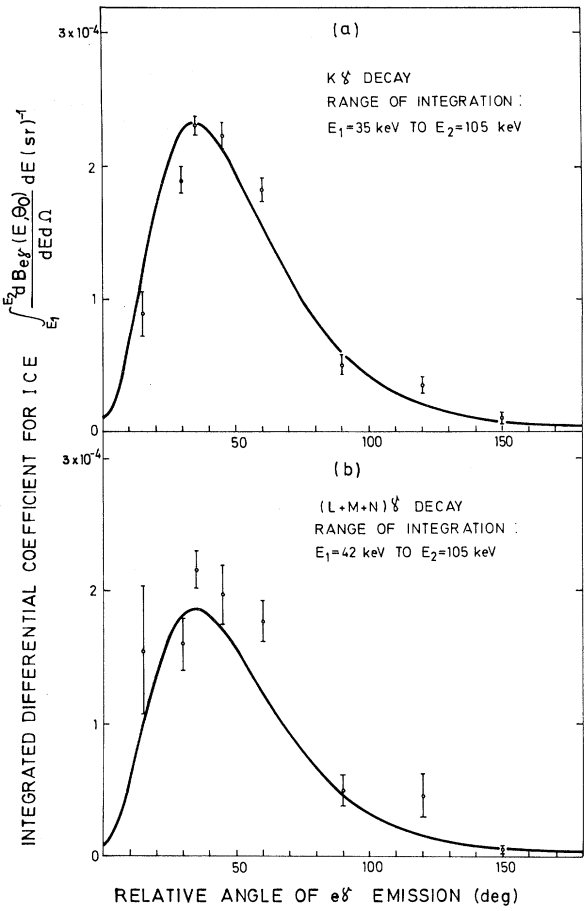

FIG. 4. Angular distribution of photons for (a) $K\gamma$ decay and (b) $(L+M+N)\gamma$ decay in ^{113}In. The full curves show the results derived from the theory of Spruch and Goertzel.

TABLE IV. Angular distribution of photons (in units of 10^{-4} sr^{-1}) in the $K\gamma$ and $(L+M+N)\gamma$ decays of the 392-keV state in ^{113}In.

Θ_0 (deg)	$\int_{35\text{ keV}}^{105\text{ keV}} [dB_{K\gamma}(E,\Theta_0)/dE\,d\Omega]dE$	$\int_{42\text{ keV}}^{105\text{ keV}} [dB_{(L+M+N)\gamma}(E,\Theta_0)/dE\,d\Omega]dE$
15	0.89± 0.17	1.56± 0.48
30	1.90± 0.07	1.60± 0.20
35	2.31± 0.06	2.16± 0.13
45	2.24± 0.10	1.98± 0.23
60	1.83± 0.08	1.77± 0.14
90	0.51± 0.06	0.50± 0.11
120	0.36± 0.05	0.46± 0.16
150	0.11± 0.04	0.06± 0.02

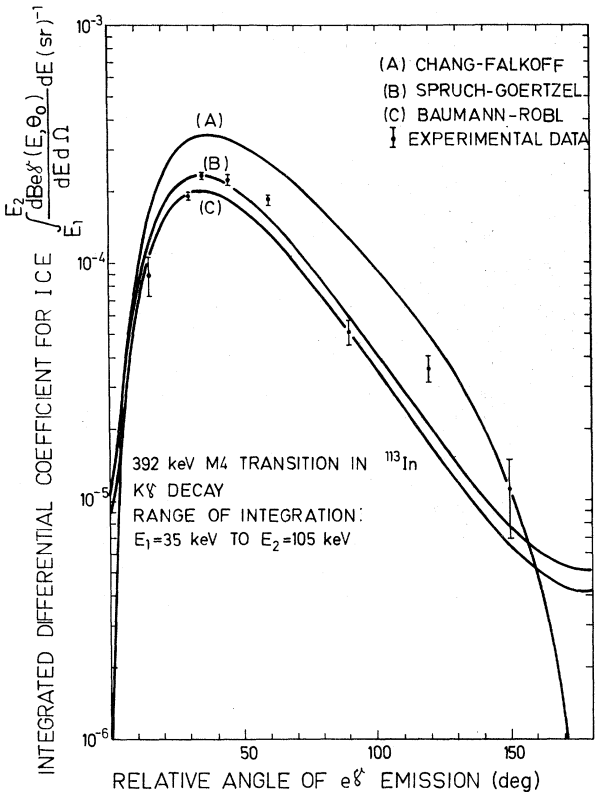

FIG. 5. Comparison of the experimental angular distribution of $K\gamma$ decay in ^{113}In with the theoretical distributions of (A) Chang and Falkoff, (B) Spruch and Goertzel, and (C) Baumann and Robl.

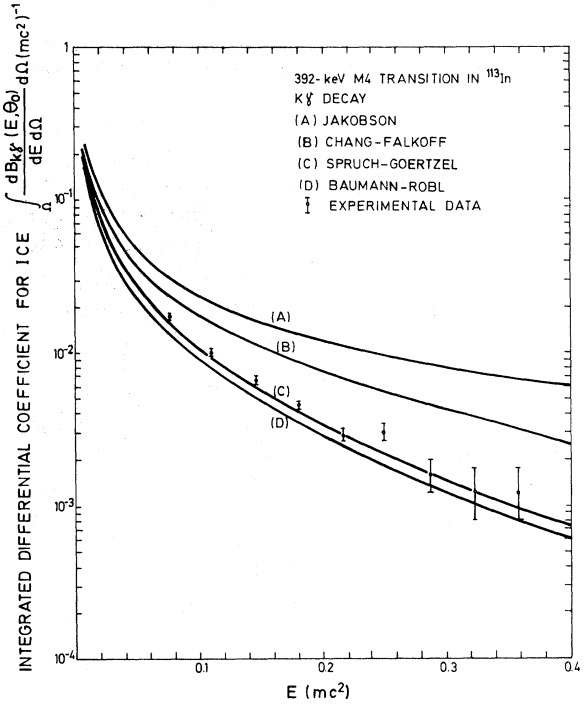

FIG. 6. Comparison of the experimental energy distribution of $K\gamma$ decay in ^{113}In (obtained by integration over the whole solid angle) with the theoretical distributions of (A) Jakobson, (B) Chang and Falkoff, (C) Spruch and Goertzel, and (D) Baumann and Robl.

value[14] of 0.438 ± 0.008 and of the theoretical value of 0.44 obtained from the tables of Hager and Seltzer.[15] This means that the transition probabilities for the ICE, as given by Spruch and Goertzel, are underestimated by the same factor. It seems that the differential coefficients for the ICE depend only on the states of the converted electron, and the rate of $e\gamma$ decay is very nearly proportional to the rate of emission of conversion electrons.

In calculating radiation losses in internal conversion Baumann and Robl neglected some terms which were estimated to give a small contribution when the photon and electron momentum, measured in natural units, were much larger than $Z/137$. Formally, their theory can be described as the scattering of a free electron, initially at rest, on a modified multipole field of the nucleus in which a bremsstrahlung quantum is emitted. The intermediate and final states of the electron were approximated by plane waves. Explicit formulas were given for electric and magnetic multipole transitions. Their results agree closely with the results of Spruch and Goertzel.

Jakobson[8] calculated the energy distribution of the ICE in a nonrelativistic approximation, assuming that the transition energy was small compared with the rest energy of the electron. In this approximation $e\gamma$ decay proceeds as a two-step process: an electron conversion followed by the emission of a bremsstrahlung quantum.

The results for the $K\gamma$ decay of ^{113}In, derived

TABLE V. Energy distribution of photons [in units of 10^{-3} $(mc^2)^{-1}$] obtained by integrating the experimental angular distribution over the whole solid angle in the $K\gamma$ decay of ^{113}In.

Photon energy interval (keV)	$\int_\Omega (dB_{K\gamma}(E,\Theta_0)/dE\,d\Omega)d\Omega$
30–48	17.2 ± 0.7
48–66	10.0 ± 0.4
66–84	6.62 ± 0.36
84–102	4.59 ± 0.31
102–120	2.89 ± 0.30
120–138	3.03 ± 0.36
138–156	1.61 ± 0.39
156–174	1.23 ± 0.41
174–192	1.24 ± 0.52
192–210	−0.49 ± 0.63

from the above-mentioned theories, are compared with the experimental angular and energy distributions in Figs. 5 and 6. The angular distributions obtained by integrating the differential coefficients for $K\gamma$ decay over an energy interval from 35 to 105 keV are presented in Table IV and compared with the theoretical values in Fig. 5.

The values of the energy distribution obtained by integrating the experimental values of $K\gamma$ coefficients are given in Table V and compared with the theoretical energy distributions (also integrated over the whole solid angle) in Fig. 6.

Nuclear intermediate states

"Nuclear" $e\gamma$ decay has also been studied by several authors.[16-18] Grechukhin[18] gave general expressions for the calculation of differential transition probabilities integrated over the solid angle for different combinations of multipoles of the emitted electron and photon.

$e\gamma$ two-quantum decay proceeds via many $(\gamma L_1, e L_2)$ channels. These should satisfy the conservation laws of angular momentum and parity

$$\vec{L}_1 + \vec{L}_2 = \vec{I}_1 - \vec{I}_2$$

and

$$\pi(L_1)\pi(L_2) = \pi(I_1)\pi(I_2)\,, \tag{3}$$

where $\vec{L}_1$ and $\vec{L}_2$ and $\pi(L_1)$ and $\pi(L_2)$ are the angular momenta and parities of the emitted quanta, respectively, $\vec{I}_1$ and $\vec{I}_2$ and $\pi(I_1)$ and $\pi(I_2)$ are the angular momenta and parities of the initial and final states of the nuclei, respectively. The interference of different combinations of multipoles is possible. However, after the integration over the solid angle the interference terms vanish, and the total transition probability is a sum of transition probabilities of all $(\gamma L_1, e L_2)$ channels.

According to Grechukhin[18] the transition probability of $e\gamma$ decay in which a photon of energy ω and an electron (originating from the qth shell) of energy $W-\omega$ are emitted is equal to (in units $\hbar = c = m_e = 1$)

$$\frac{dT'_{e\gamma}(\omega,q)}{d\omega} = \frac{e^2}{\pi}\left(\frac{1}{MR_0}\right)^2 \frac{\omega^{2L+1}R_0^{2L}}{[(2L+1)!!]^2}\left(\frac{2L+1}{L+1}\right)\Omega(q, W-\omega)\,|\langle I_2\|(ML\omega EOW-\omega)L\|I_1\rangle|^2$$
$$+\sum_{L_1L_2}\frac{e^4}{(MR_0)^2}\frac{2}{\pi}\frac{\omega^{2L_1+1}(W-\omega)^{2L_2+1}R_0^{2L}}{[(2L_1+1)!!(2L_2+1)!!]^2}\left[\frac{(2L_1+1)}{L_1+1}\frac{(L_2+1)}{L_2}\alpha(EL_2;q,W-\omega)\,|\langle I_2\|(ML_1\omega EL_2W-\omega)L\|I_1\rangle|^2\right.$$
$$\left.+\left(\frac{L_1+1}{L_1}\frac{2L_2+1}{L_2+1}\right)\beta(ML_2;q,W-\omega)\,|\langle I_2\|EL_1\omega ML_2W-\omega)L\|I_1\rangle|^2\right]. \tag{4}$$

Here $e^2 = 1/137$, $M \approx 1837$ is the average nucleon mass, $R_0 = 0.43A^{1/3}\,e^2$ is the nuclear radius (A being the nucleon number), L_1 and L_2 are the angular momenta of the emitted photon and electron, respectively, and L is the multipolarity of the direct transition. W is the transition energy, $\Omega(q, W-\omega)$ is the electronic factor[19] of an $E0$ nuclear transition involving the qth atomic shell, and $\alpha(EL_2; q, W-\omega)$ and $\beta(ML_2; q, W-\omega)$ are the electron conversion coefficients for EL_2 and ML_2 transitions for the qth shell and energy $W-\omega$. The first term in the sum gives the contribution of the $(\gamma L, eE0)$ channel, and the rest gives the contribution of other $(\gamma L_1, e L_2)$ channels. Only the lowest combinations of multipolarities are taken into account, since the sum is restricted by the condition $L_1 + L_2 = L = |I_1 - I_2| = \kappa$.

The reduced matrix elements of $e\gamma$ decay can be expressed by means of the reduced matrix elements of single-quantum decays

$$\langle I_2\|(L_1\omega L_2W-\omega)\kappa\|I_1\rangle = \left[\sum_{kI_k} U(I_2I_1L_2L_1;\kappa I_k)\frac{\langle I_2\|L_2\|I_k\rangle\langle I_k\|L_1\|I_1\rangle}{E_k - E_2 - (W-\omega)}\right.$$
$$\left.+(-1)^{\kappa-L_1-L_2}\sum_{sI_s} U(I_2I_1L_1L_2;\kappa I_s)\frac{\langle I_2\|L_1\|I_s\rangle\langle I_s\|L_2\|I_1\rangle}{E_s - E_2 - \omega}\right]. \tag{5}$$

Here $U(abcd;ef)$ are normalized Racah coefficients, I_k and I_s and E_k and E_s are the angular momenta and energies of nuclear intermediate states, respectively, and E_2 is the energy of the final state of the nucleus. The summation should be made over all intermediate states which are above the

initial state of the nucleus, and which satisfy the conservation laws (3). Equation (5) is valid for all channels, including the $(\gamma L, eE0)$ channel, and therefore the indices (ML, EL) are omitted.

The reduced matrix elements in Eq. (5) can be calculated from the formulas (also in units $\hbar = c = m_e = 1$)

$$T_\gamma(EL;\omega;I_i \to I_k) = 2e^2 \frac{\omega^{2L+1}R_0^{2L}}{[(2L+1)!!]^2} \frac{L+1}{L} |\langle I_k \| EL \| I_i\rangle|^2,$$

$$T_\gamma(ML,\omega;I_i \to I_k) = \frac{2e^2}{(MR_0)^2} \frac{\omega^{2L+1}R_0^{2L}}{[(2L+1)!!]^2} \frac{2L+1}{L+1} |\langle I_k \| ML \| I_i\rangle|^2, \quad (6)$$

$$|\langle I_k \| L \| I_i\rangle|^2 = \frac{2I_k+1}{2I_i+1} |\langle I_i \| L \| I_k\rangle|^2,$$

where $T_\gamma(EL;\omega, I_i \to I_k)$ and $T_\gamma(ML;\omega, I_i \to I_k)$ are the transition probabilities of single-quantum EL and ML transitions between the states $I_i \to I_k$ with the transition energy $\omega = E_i - E_k$.

The reduced matrix elements were calculated using the single-particle model estimates of Moszkowsky.[20] The $(\gamma L, eL0)$ channel was neglected. The following intermediate states of ^{113}In were considered: $\frac{3}{2}^-$(0.647 MeV), $\frac{5}{2}^+$(1.024 MeV), $\frac{3}{2}^+$(1.029 MeV), and $\frac{7}{2}^+$(1.194 MeV). These states have recently been studied both experimentally and theoretically.[21] The internal conversion coefficients were obtained by interpolation from the tables of Hager and Seltzer.[15]

For the sake of consistency, the internal conversion transition probability for the direct transition, i.e., of the 392-keV $M4$ transition in ^{113}In, for the qth atomic shell, was calculated by the formula

$$T_q(M4) = \beta_q(M4) T_\gamma(M4). \quad (7)$$

Here the values for the internal conversion coefficient $\beta_q(M4)$ were taken from the tables of Hager and Seltzer, and the γ-ray transition probability $T_\gamma(M4)$ was calculated from Moszkowsky's single-particle model.

A comparison of the energy distributions of photons obtained by integration over all directions of emission of the theoretical "electronic" and "nuclear" $e\gamma$ differential coefficients is shown in Fig. 7. The differential coefficient for nuclear $K\gamma$ decay, $(1/T_K)dT'_K(E_\gamma)/dE_\gamma$, increases strongly with energy, while a broad maximum appears for $L\gamma$ and $M\gamma$ decays. At energies close to the maximum photon energy the nuclear $K\gamma$ coefficients, according to the results, become larger than the internal Compton coefficients. Therefore, attempts to determine nuclear $K\gamma$ decay should be made at large angles of relative emission and by including large

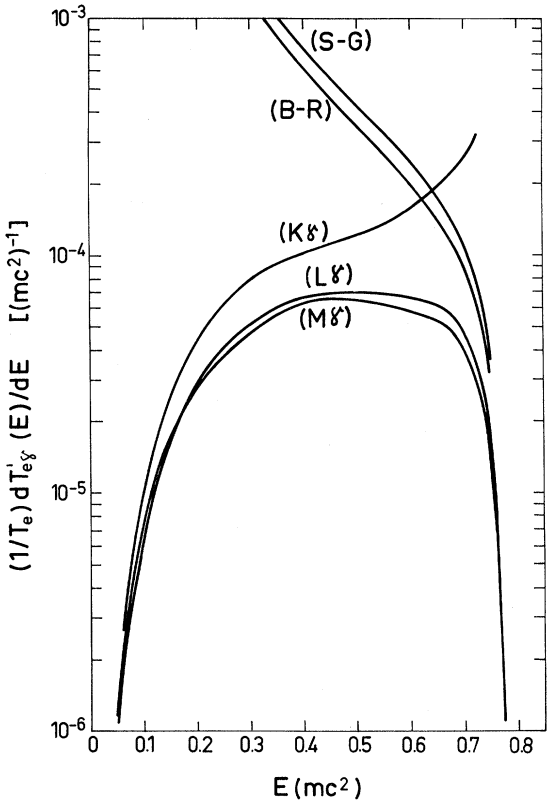

FIG. 7. Comparison of energy distributions in $e\gamma$ decay in ^{113}In due to "electronic" and "nuclear" intermediate states (integrated over the whole solid angle). The ICE distributions were calculated from the theories of Spruch and Goertzel (S-G) and Baumann and Robl (B-R). The distributions calculated from the theory of Grechukhin for "nuclear" $e\gamma$ decay for K-, L-, and M-shell electrons are marked by $(K\gamma)$, $(L\gamma)$, and $(M\gamma)$, respectively.

photon (and, of course, low electron) energies. According to our experience, a measurement with the required sensitivity could be performed with the currently available experimental techniques, but it would be difficult and very long.

Integrating these coefficients, we obtained the following values for the transition probabilities:

$$T'_{K\gamma}(E_\gamma = 35 \text{ to } 105 \text{ keV})/T_K = 3.4\times10^{-6},$$

$$T'_{L\gamma}(E_\gamma = 42 \text{ to } 105 \text{ keV})/T_L = 2.2\times10^{-6},$$

$$T'_{M\gamma}(E_\gamma = 42 \text{ to } 105 \text{ keV})/T_M = 2.3\times10^{-6}.$$

Comparison of these values with the results of measurements and with the values calculated from the theory of Spruch and Goertzel and from the theory of Baumann and Robl shows that the contribution of nuclear $e\gamma$ decay in the region of measurements is negligible.

ACKNOWLEDGMENTS

The authors thank K. Pisk and A. Ljubičić for many fruitful discussions, the Electronics Department for the construction and maintenance of the three-dimensional analyzer, Mrs. N. Ilakovac for the preparation of silicon surface-barrier detectors, and I. Čelig for his help with the equipment in the laboratory.

---

†Research supported by the Council for Scientific Research of S. R. Croatia, Zagreb, Yugoslavia.

[1]M. Jurčević, K. Ilakovac, and Z. Krečak, Phys. Rev. C 9, 1611 (1974).

[2]L. Spruch and G. Goertzel, Phys. Rev. 94, 1671 (1954).

[3]E. J. Seykora, Ph.D. thesis, North Carolina State University, Raleigh, 1968 (unpublished).

[4]H. Aiginger, Z. Phys. 197, 8 (1966).

[5]V. K. Baumann and H. Robl, Z. Naturforsch. 9a, 511 (1954).

[6]C. S. Wang Chang and D. L. Falkoff, Phys. Rev. 76, 365 (1949).

[7]E. P. Cooper and P. Morrison, Phys. Rev. 57, 862 (1940).

[8]A. M. Jakobson, Zh. Eksp. Teor. Fiz. 29, 703 (1955) [transl.: Sov. Phys.—JETP 2, 751(L) (1965)].

[9]E. G. Melikian, Zh. Eksp. Teor. Fiz. 31, 1088 (1956) [transl.: Sov. Phys.—JETP 4, 930(L) (1957)].

[10]F. Yanoukh, Zh. Eksp. Teor. Fiz. 38, 180 (1960) [transl.: Sov. Phys.—JETP 11, 131 (1960)].

[11]H. T. Williams, Jr., Ph.D. thesis, University of Virginia, 1967 (unpublished).

[12]E. G. Drukarev, Yad. Fiz. 17, 342 (1973) [transl.: Sov. J. Nucl. Phys. 17, 174 (1973)].

[13]T. Lindqvist, B. G. Pettersson, and K. Siegbahn, Nucl. Phys. 5, 47 (1958); E. Fuschini, C. Maroni, and P. Veronesi, Nuovo Cimento 26, 831 (1962); 41B, 252 (1966); A. Ljubičić, B. Hrastnik, K. Ilakovac, V. Knapp, and B. Vojnović, Phys. Rev. 187, 1512 (1969); A. Ljubičić, B. Hrastnik, K. Ilakovac, M. Jurčević, and I. Basar, Phys. Rev. C 3, 824 (1971).

[14]C. M. Lederer, J. M. Hollander, and I. Perlman, *Table of Isotopes* (Wiley, New York, 1968), 6th ed.

[15]R. S. Hager and E. C. Seltzer, Nucl. Data A4, 1 (1968).

[16]M. L. Goldberger, Phys. Rev. 73, 1119 (1948).

[17]J. Eichler, Z. Phys. 160, 333 (1960).

[18]D. P. Grechukhin, Yad. Fiz. 4, 42 (1966) [transl.: Sov. J. Nucl. Phys. 4, 30 (1967)].

[19]E. L. Church and J. Weneser, Phys. Rev. 103, 1035 (1956).

[20]S. A. Moszkowski, in *Alpha-, Beta-, and Gamma-Ray Spectroscopy*, edited by K. Siegbahn (North-Holland, Amsterdam, 1965), p. 863.

[21]E. M. Bernstein, G. G. Seaman, and J. M. Palms, Nucl. Phys. A141, 67 (1970); S. Sen, *ibid.* A191, 29 (1972); H. J. Kim and R. L. Robinson, Phys. Rev. C 9, 767 (1974); R. G. Markham and H. W. Fulbright, *ibid.* 9, 1633 (1974).